NAP-2014

The Study of the Alginate / Hydroxyapatite Composites Structural Properties

V.N. Kuznetsov*, L.B. Sukhodub, L.F. Sukhodub

Sumy State University, 2, Rymsky Korsakov Str., 40007 Sumy, Ukraine

This paper describes the synthesis of sodium alginate (Alg) / hydroxyapatite (HA) composites and the influence of the presence of Alg on HA crystallization. Such composites become rather widespread in recent years, and are used in medicine generally for the controlled drug delivery. In one's case, Alg is used as the functional and cost-effective replacement of the collagen for the creation of implants similar to the natural bone. It was shown that the presence of Alg and the increase of its concentration leads to the decrease of the HA crystallinity thus providing an ability to control its levels in the resulting product. The FTIR studies confirm the incorporation of Alg in the Alg / HA composite structure.

Keywords: Alginate, Hydroxyapatite, XRD, SEM, EDS, FTIR.

PACS numbers: 87.85.J–, 87.64.Bx, 87.64.Ee

1. INTRODUCTION

This paper describes the synthesis of sodium alginate (Alg) / hydroxyapatite (HA) composites and the influence of the presence of Alg on HA crystallization. Such composites become rather widespread in recent years, and are used in medicine generally for the controlled drug delivery [1-3].

Alginate is non-toxic, biodegradable, and biocompatible. It's a linear watersoluble polysaccharide consisting of monomeric units of 1-4 linked α-D-mannuronate (M) and β-L-guluronate (G) at different proportions in the chain, which is isolated from brown algae and can be synthesized from microorganisms [4]. It is used as the wound dressing material for the treatment of acute or chronic wounds, the basis of bacterial biofilms, for making hydrogels for cell encapsulation [5].

In one's case, Alg is used as the functional and cost-effective replacement of the collagen for the creation of implants similar to the natural bone [6].

2. MATERIALS AND METHODS

2.1 Materials

The synthesis of composite materials based on calcium phosphates (including HA) containing sodium alginate consists of the following steps.
1. The 1 wt. % sodium alginate water solution was prepared by the Alg dissolution in the deionized water using the shaker at 37 ºC for 4 hours.
2. The derived (in the 1st step) solution of the required quantities providing 25 % and 50 % of Alg was mixed with 0,1 M sodium dehydrophosphate NaH_2PO and 0,167 M calcium acetate $Ca(CH_3COO)_2$ solutions.
3. The addition of 18 wt. % caustic soda water solution was led to the $9,75 \div 10$ suspension (derived in the 2nd step) pH levels.
4. The suspension (derived in the 3rd step) was mixed in the shaker at 254 rpm and 70 ºC for 2 hours and left for the 1 day aging.
5. After the thorough washing till 7,4 cleaning water

pH value the part of the product was dried in the exsiccator at 37 ºC, the other one was freeze-dried.

Such materials were used: sodium alginate (E 401) was supplied by China, analytically grade calcium acetate $Ca(CH_3COO)_2$, sodium dehydrophosphate NaH_2PO_4, and sodium hydroxide (NaOH) were supplied by Merck.

2.2 Methods

The crystallinity and structure of the synthesized samples were examined using an X-ray diffractometer DRON-3 (Bourevestnik, Inc., Saint-Petersburg, Russian Federation) connected to a computer-aided system for the experiment control and data processing. The current and the voltage of the X-ray tube were 20 mA and 40 kV respectively. All experimental data was processed by means of the program package DIFWIN-1 (Etalon PTC, Ltd., Moscow, Russian Federation). Identification of crystal phases was done using a JCPDS card catalog (Joint Committee on Powder Diffraction Standards).

The crystallite sizes L were calculated using the Scherrer equation [7]:

$$L = \frac{K\lambda}{\beta \cos\theta},\qquad(2.1)$$

where K is the form coefficient ($K = 1$), λ is the wavelength, β is the peak broadening, θ is the diffraction angle.

The quantitative phase analysis was done using the reference intensity ratio (RIR) method [8]:

$$C_i = \left(\frac{K_i I_i^{rel}}{I_i} \sum_{i=1}^{n} \frac{I_i}{K_i I_i^{rel}} \right)^{-1},\qquad(2.2)$$

where C_i is the concentration of the i-phase, K_i is the corundum number of the i-phase, I_i is the peak integral intensity of the i-phase, I_i^{rel} is the peak relative intensity of the i-phase.

The Ca/P ratio was calculated using method described in [9]:

---

* vkuznetsov.ua@gmail.com

$$\frac{Ca}{P} = \frac{10 \cdot (100 - C_{TCP}) / M_{HAP} + 3 \cdot C_{TCP} / M_{HAP}}{6 \cdot (100 - C_{TCP}) / M_{HAP} + 2 \cdot C_{TCP} / M_{HAP}}, (2.3)$$

where C_{TCP} is the TCP phase concentration (%), M_{HAP} is the molar mass.

The scanning electronic microscopy (SEM) with energy dispersive spectroscopy (EDS) was used for studying the morphology and the elemental composition of the samples. The beam voltage was 20 kV.

FTIR spectroscopy was used to study the incorporation of Alg in the HA structure.

3. RESULTS AND DISCUSSION

The derived results show that the major calcium phosphate phase in all cases is HA (JCPDS 9-432). The presence of Alg in the solution reduces the crystallinity of the resulting product. The crystallinity decreases with the increase of the Alg concentration (see Fig. 1). At 50 % nanocrystalline HA is formed (see Fig. 1b). The mean crystallite sizes of the HA phase in (0 0 4) plane of the non-heat treated samples are ~ 22 nm. This can be explained due to the different contribution of the microstrains in the samples peak broadening.
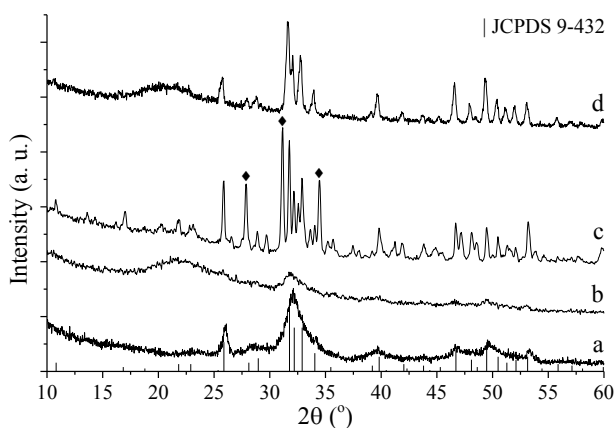

Fig. 1 – X-Ray diffraction spectra of Alg / HA composites: a – 25 % Alg, b – 50 % Alg, c – 25 % Alg heat treated at 800 ᵒC for 1 hour, d – 50 % Alg heat treated at 800 ᵒC for 1 hour. Major TCP peaks are marked with ♦

After the heat treatment at 800 ᵒC for 1 hour the crystallinity of both samples grew at different amounts. In case of the 25% Alg sample (see Fig. 1c) the HA peak packet at 2θ ~ 31,5ᵒ ÷ 33,5ᵒ is resolved very well. Its phase composition consists of two phases – hydroxyapatite and tricalcium phosphate (TCP) which indicates that the crystallization of nonstehiometric apatite has occurred

The other sample (see Fig. 1d) shows the presence of the only phase – HA with its main peak packet resolved notably worse than the previous one.

The phase concentrations and approximate Ca/P ratios of the studied samples are shown in Table 1.

The micrograph of the composite structure and its EDS spectrum are shown in Fig. 2.

Table 1 – Phase concentrations and Ca / P ratios of Alg / HA composites

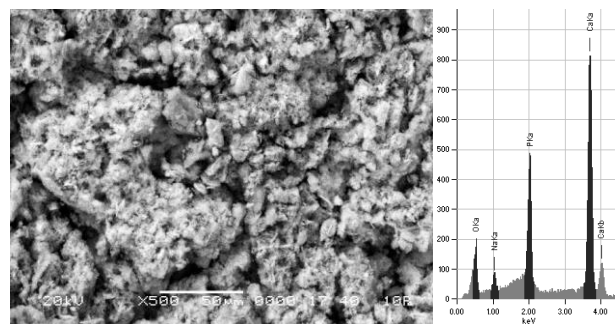| Sample	HA		TCP		Ca/P, at. %
	JCPDS	Concen-tration, %	JCPDS	Concen-tration, %	
25 % Alg	9-432	50	9-169	50	1,62
50 % Alg	9-432	100	–	–	1,67

Fig. 2 – SEM picture and EDS spectrum of 25 % Alg / HA composite

The FTIR spectra show the presence of both Alg and HA characteristic vibrations in the resulting product (see Fig. 3).
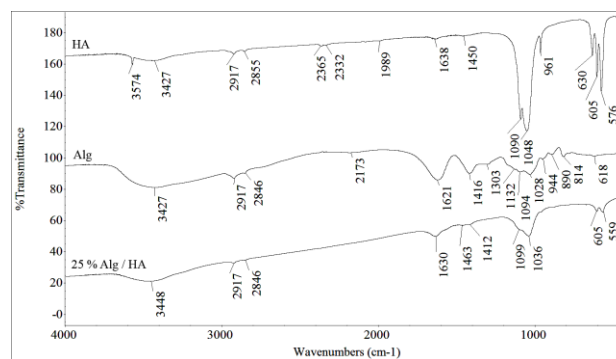

Fig. 3 – FTIR spectra of precursors (Alg and HA) and the resulting 25 % Alg / HA composite

4. CONCLUSIONS

The major calcium phosphate phase in all alginate / hydroxyapatite non-heat treated samples was HA with mean crystallite sizes ~ 20 nm. The presence of Alg in the solution reduces the crystallinity of the resulting product. The crystallinity decreases with the increase of the Alg concentration. This corresponds to the results [5,10]. After heating at 800 ᵒC for 1 hour the 25 % Alg sample, the phase composition included two phases: HA and TCP, but the 50% Alg sample after the same treatment showed the presence of the single HA phase. This result is very promising and requires further studies to understand Alg role in this specific crystal transformation for such kind of nanocomposites.

REFERENCES

1. J. Zhang, Q. Wang, A. Wang, *Acta Biomater.* **6**, 445 (2010).
2. C.-H. D. Chen, C.-C. Chen, M.-Y. Shie, C.-H. Huang,

S.-J. Ding, *Mater. Sci. Eng.* **C31**, 334 (2011).
3. C.C. Ribeiro, C.C. Barrias, M.A. Barbosa, *Biomaterials* **25**,

4363 (2004).
4. M. Alboofetileh, M. Rezaei, H. Hosseini, M. Abdollahi, *Food Control* **36**, 1 (2014).
5. S.N. Pawar, K.J. Edgar, *Biomaterials* **33**, 3279 (2012).
6. L.F. Sukhodub, G.O. Yanovska, L.B. Sukhodub, V.M. Kuznetsov, O.S. Stanislavov, *J. Nano- and Electron. Physics* **6** (1), 01001 (2014).
7. H.P. Klug, L.E. Alexander, *X-Ray Diffraction Procedures: For Polycrystalline and Amorphous Materials* (New York: Wiley: 1974).
8. F.H. Chung, *J. Appl. Crystallogr.* **8**, 17 (1975).
9. S. Raynaud, E. Champion, D. Bernache-Assollant, J.-P. Laval, *J. Am. Ceram. Soc.* **84** No2, 359 (2001).
10. P. Malkaj, E. Pierri, E. Dalas, *J. Mater. Sci.-Mater. M.* **16** No8, 733 (2005).